**Title: Brain connectivity during Alzheimer's disease progression and its cognitive impact in a transgenic rat model.**

**Author names and affiliations:** Emma Muñoz-Moreno[a]*, Raúl Tudela[b,a], Xavier López-Gil[a], Guadalupe Soria[a,b;]

[a] Experimental 7T MRI Unit, Institut d'Investigacions Biòmediques August Pi i Sunyer (IDIBAPS), Barcelona, 08036, Spain

[b]Consorcio Centro de Investigación Biomédica en Red (CIBER) de Bioingeniería, Biomateriales y Nanomedicina (CIBER-BBN), Group of Biomedical Imaging, University of Barcelona, Barcelona, 08036, Spain

**Corresponding author**: emunozm@clinic.ub.es

**E-mail addresses:** raul.tudela@ub.edu, xavier.lopez@idibaps.org, guadalupe.soria@idibaps.org

**Abstract**

It is known that brain alterations associated to Alzheimer's disease (AD) start decades before its diagnose. However, the understanding of the disease progression is still an open issue, due partly to the difficult to follow-up patients from asymptomatic to advanced stages. In this sense, animal models become essential to improve the characterization of AD from early to symptomatic stages. In the present work, transgenic TgF344-AD rats were evaluated longitudinally, every 3 months, starting when the animals were 6 months of age. At each time point, cognitive abilities were evaluated by a memory-related task, the delayed non-matched-to-sample task (DNMS), and functional and structural connectivity were analysed based on magnetic resonance imaging (MRI). Brain networks were estimated and characterized by graph metrics. Differences between connectivity and its evolution with age in transgenic and control animals were evaluated, as well as the relationship between brain networks and cognition. Results shown alterations in the structural network of transgenic animals since the first evaluated time point. Likewise, aging had a significant effect in the network metrics of these animals, while such an effect was not observed in the control group. The relationship between cognition and connectivity differed between groups. While DNMS results were influenced by the structural brain network in transgenic animals, functional network has a major effect in the performance of control subjects. This different relationship was present even though effects of group or interaction between group and age were not significant in neither the functional networks or cognitive performance,

In summary, the connectivity analysis of TgF344-AD provides a highly translational approach to characterize early stages and progression of AD. The results confirm findings observed in human populations at risk of AD and provide new insights in the evolution of brain networks affected by the disease. Results support the idea of AD as a continuum and the disconnection hypothesis, pointing to different organization of structural brain network whose consequences in cognitive impairment could be compensated by functional connectivity until advanced stages of AD,

suggesting the influence of cognitive reserve in the preservation of functional abilities in AD subjects.

**Keywords:** Alzheimer's disease continuum, animal models, TgF344-AD, connectomics, brain networks, longitudinal evolution.

## 1. INTRODUCTION

Alzheimer's disease (AD) is a neurodegenerative disease related to most cases of dementia in elderly population. Brain damage associated to AD starts decades before the symptomatic onset and clinical diagnose, which has led to consider AD as a continuum (Dubois et al., 2016; Jack et al., 2018). In this line, studies performed on AD risk population such as carriers of apolipoprotein E (*APOE*)-ε4 or *rs405509* alleles have detected brain differences between these subjects and control subjects in elderly (Chen et al., 2015; Reiter et al., 2017; Shu et al., 2015) and middle-age healthy population (Cacciaglia et al., 2018; Habib et al., 2017; Mak et al., 2017; ten Kate et al., 2016). Notwithstanding these evidences, the disease progression is not completely understood, partly due to the challenges in the identification of at-risk population and the time required to follow-up them from middle-age to the eventual advanced phase of AD. In this sense, animal models provide a helpful approach to evaluate the development of AD from early to advanced stages (Do Carmo and Cuello, 2013; Galeano et al., 2014; Leon et al., 2010; Sabbagh et al., 2013). AD is related with the presence and interplay of both amyloid plaques and neurofibrilary tangles and therefore animal model should replicate these two aspects to lead to successful and translational results (Drummond and Wisniewski, 2017). For instance, TgF344-AD rats progressively manifest most pathological hallmarks of the disease including amyloid plaques, tau pathology, oligomeric amyloid β (Aβ),

neuronal loss and behavioral impairment (Cohen et al., 2013; Drummond and Wisniewski, 2017), which makes it a very suitable model to evaluate AD progression during aging.

Along with the choice of appropriate animal models, the use of replicable techniques in experimental and clinical research can improve translationality (Sabbagh et al., 2013). This is a crucial point given the high failure rates in the translation between preclinical and clinical trials reported in drug research for AD (Drummond and Wisniewski, 2017; Windisch, 2014). Neuroimaging techniques have been extensively used to identify alterations associated to the disease in a non-invasive way and can be applied in both animal and human cohorts (Sabbagh et al., 2013). In the search for AD biomarkers, magnetic resonance imaging (MRI) has represented a helpful technique to characterize in-vivo brain changes during AD progression (Jack et al., 2015), such as atrophy (Frisoni et al., 2010) or tissue changes (Weston et al., 2015). In addition, MRI can be used to identify and describe structural and functional brain networks. For this reason it has been used to investigate and support the hypothesis of AD as a disconnection syndrome (Brier et al., 2014a; Gomez-Ramirez and Wu, 2014; Palesi et al., 2016; Xie and He, 2012), suggesting that cognitive decline in AD is related to functional or structural disconnection between regions rather than localized changes in specific isolated brain areas. Thus, impairment in structural connectivity associated to AD has been described based on gray matter patterns evaluated in structural MRI or, mainly, based on the fiber tract estimations obtained from diffusion weighted MRI (Daianu et al., 2013; Fischer et al., 2015; Lo et al., 2010; Wee et al., 2011). Likewise, functional disconnection has been evaluated using resting-state functional MRI (rs-fMRI) and graph theory to estimate and quantify functional network (Brier et al., 2014b; Sanz-Arigita et al., 2010; Supekar et al., 2008); identifying resting-state networks using independent component analysis (Badhwar et al., 2017); or characterizing connectivity between a specific region and the rest of the brain (Gour et al., 2014). Indeed, alterations in structural and functional brain network properties have been described in

TgF344-AD animals at early ages (5-6 months) (Muñoz-Moreno et al., 2018) as well as differences in functional connectivity of specific regions at several time points from 6 to 18 months (Anckaerts et al., 2019).

In the present study, we investigated how the disease progression affects both structural and functional brain networks and its effects in cognitive abilities. In this sense, we evaluated how the connectivity impairments observed in young TgF344-AD animals in our previous work (Muñoz-Moreno et al., 2018) evolve during aging. To do this, a longitudinal analysis of brain connectivity was performed based on MRI acquisitions repeated every 3 months from 6 to 18 months of age in a cohort of TgF344-AD rats, which was compared with control animals. Cognitive skills were also evaluated every 3 months to test the impact of connectivity alterations in cognition. Therefore, this work aims to contribute to the understanding of AD progression and its association with cognitive decline from the perspective of the disease as a disconnection syndrome.

## 2. Materials and Methods

### *2.1. Subjects*

The experiments were performed in a cohort of 18 male rats including nine TgF344-AD animals (Cohen et al., 2013) and nine wild-type Fisher rats. The animals were housed in cages under controlled temperature (21 ± 1ºC) and humidity (55 ± 10%) with a 12 hour light/12 hour dark cycle. Food and water were available *ad libitum* during all the experiment, except during behavioral test periods as explained below. At 2 months of age, animals start a cognitive training to perform delay non-matched sample (DNMS) task. Once the learning criteria was achieved, their performance in DNMS was evaluated and the first MRI scan was acquired. Afterwards, two weeks of DNMS sessions followed by MRI acquisition were repeated every three months resulting in five evaluated time points. Table 1 shows the details on sample size and age.

| | CTR | | AD | |
|---|---|---|---|---|
| | N | AGE (months) | N | AGE (months) |
| Time point 1 | 8/5* | 5.33±0.3 | 8/7* | 6.33±1.22 |
| Time point 2 | 9 | 9.2±0.5 | 8 | 8.67±0.2 |
| Time point 3 | 7 | 11.3±0.22 | 9 | 11.3±0.03 |
| Time point 4 | 8 | 14.9±0.425 | 9 | 14.87±0.03 |
| Time point 5 | 8 | 17.92±0.52 | 6 | 18.03±0.62 |

***Table 1.*** Sample size and age (median ± interquartile range) at each of the 5 acquisitions. Sample size in time point 1 is different in the structural and functional analysis (*corresponds to the number of rs-fMRI acquisitions). Variability in the age of acquisition at the first time point is due to differences in the cognitive training duration. The age difference between groups was not significant.

Animal work was performed following the local legislation (Decret 214/1997 of July 20th by the Department d'Agricultura, Ramaderia i Pesca de la Generalitat de Catalunya) under the approval of the Experimental Animal and Ethical Committee of the University of Barcelona (CEEA) and in compliance with European legislation.

### *2.2. Cognitive function evaluation*

Every three months, working memory was evaluated by DNMS test, following the procedure described in (Muñoz-Moreno et al., 2018). DNMS was carried out in isolated operant chambers (Med Associates, USA), equipped with a pellet dispenser and three retractable levers, two of them in the wall where the pellet is (right and left levers) and the other in the opposite side (center lever). During the testing weeks, rats were food-deprived, receiving 75% of the usual food intake. In brief, DNMS requires the animal to press the levers following a specific sequence to obtain a pellet. First, in the sample phase, right or left lever appeared and after the animal pressed it, a delay randomly

timed between 1 and 30 seconds started, after which the center lever appeared. When the animal pressed it both right and left levers were extended again. Correct response required a press on the lever opposite to the presented in the sample phase. Each DNMS session finished after 90 minutes or when 90 trials were completed. The number of trials and percentage of correct responses were recorded.

Before the first test, animals underwent an habituation and training phase to acquire the required skills. This phase started when the animals were two month old and finished when they achieved an acquisition criteria as explained in (Muñoz-Moreno et al., 2018). After that, animals underwent 15 DNMS sessions (five sessions per week) to evaluate and consolidate the learnt task. At each of the following four time points, animals performed 10 DNMS sessions (two weeks).

### *2.3. Magnetic Resonance Imaging*

MRI acquisitions were performed on a 7.0T BioSpec 70/30 horizontal animal scanner (Bruker BioSpin, Ettlingen, Germany). Animals were placed in supine position in a Plexiglas holder with a nose cone for administering anesthetic gases (1.5% isoflurane in a mixture of 30% $O_2$ and 70% CO) and were fixed using tooth and ear bars and adhesive tape. The rat received a 0.5 ml bolus of medetomidine (0.05 mg/kg; s.c.) and a catheter was implanted in its back for continuous perfusion of medetomidine. Isoflurane was gradually decreased until 0% and 15 minutes after the bolus the medetomidine perfusion (0.05 mg/kg; s.c.) started at rate 1ml/hour.

The acquisition protocol included:

- T2-weighted images, acquired using a RARE sequence with effective echo time TE=35.3 ms, repetition time TR=6000 ms and RARE factor=8, voxel size = 0.12x0.12 $mm^2$, 40 slices, slice thickness=0.8 mm and field of view FoV=30x30x32 $mm^3$.

- T1-weighted images, acquired using an MDEFT protocol with TE=2 ms, TR=4000 ms, voxel size = 0.14x0.14x0.5 $mm^3$ and FoV=35x35x18 $mm^3$
- Diffusion weighted images (DWI) using a spin-echo EPI sequence with TE=24.86 ms, TR=15000 ms, four segments, 60 gradient directions with b-value=1000 s/$mm^2$ and five volumes with b-value=0 s/$mm^2$; voxel size of 0.31x0.31x0.31 $mm^3$ and FoV = 22.23x22.23x18.54 $mm^3$.
- rs-fMRI using a T2* acquisition, with the following parameters: TE=10.75 ms, TR=2000 ms, 600 volumes (20 minutes), voxel size = 0.4x0.4x0.6 $mm^3$, FoV=25.6 x 25.6 x 20.4 $mm^3$. rs-fMRI acquisition is scheduled after anatomical and diffusion MRI to ensure that isoflurane dose has been removed and the animals are sedated only by medetomidine.

### *2.4. Image processing and connectome definition*

The acquired images were processed to obtain the structural and functional connectomes following the methodology described in (Muñoz-Moreno et al., 2018). Briefly, a rat brain atlas was registered to the T2-weighted images to obtain brain masks and region parcellations (Schwarz et al., 2007). T1-weighted images were used to segment the brain into white matter (WM), gray matter (GM) and cerebrospinal fluid based on tissue probability maps registered from an atlas (Valdés-Hernández et al., 2011) to each subject brain. Parcellation and segmentation were registered from T2/T1-weighted volumes to DWI and rs-fMRI spaces to define the regions between which connectivity was assessed.

Fiber tract trajectories were estimated from DWI volumes using deterministic tractography based on constrained spherical deconvolution model, considering WM voxels as seed points. As defined in (Muñoz-Moreno et al., 2018), the structural connectome included 76 regions. Connection between

two regions was defined if at least one streamline started in one region and ended in the other. Three connectomes were considered according to the connection weight definition:

- Fractional anisotropy (FA) weighted connectome (FA-w): The connection weight between two regions is defined as the average FA in the streamlines connecting them.
- Fiber density (FD) weighted connectome (FD-w): The connection weight between two regions is computed as the number of streamlines normalized by the region volumes and the streamline length (Muñoz-Moreno et al., 2018).
- Structural binary connectome: connection weight is 1 between connected regions and zero otherwise.

rs-fMRI was processed to obtain the average time series in each of the regions of interest. Since brain activity identified by rs-fMRI has been constrained to GM (Power et al., 2017), only regions comprising GM tissue (54 regions) were considered as nodes in the functional connectome. Both weighted and binary functional connectomes were defined. The connection weight was the partial correlation between the pair of regional time series, transformed by Fisher's z-transformation. Negative correlation coefficients were excluded. Binary functional connectome was defined setting to one connections were z>0 and zero otherwise.

### *2.5. Brain network analysis*

Brain network organization was described using graph theory metrics, including degree, strength, clustering coefficient and local and global efficiency (Rubinov and Sporns, 2010).

Nodal degree measures the number of connections of a region, and nodal strength is computed as the sum of the region connection weights. Network degree and strength are the average of nodal degree and strength respectively in all the brain regions. Higher network degree/strength indicates

more or stronger connections. Global efficiency measures network integration: the ability to combine information from different regions (Rubinov and Sporns, 2010). It is inversely related with the shortest path length between each pair of nodes. Higher global efficiency characterizes stronger and faster communication through the network. Network segregation, the ability for specialized processing within densely interconnected groups of regions, was quantified by local efficiency and clustering coefficient. Local efficiency is the average in the whole network of the nodal efficiencies (efficiency of the subnetwork associated to a region). Clustering coefficient is the average of the nodal clustering coefficients, which measure the number of neighbors of a node that are also neighbors each other. High values of these metrics are related to highly segregated and connected networks.

***2.6. Statistics. Longitudinal models.***

Kruskal-Wallis tests were applied to identify statistically significant differences between transgenic and control groups at each of the five time points. Significance was defined as $p<0.05$.

The evolution of network metrics and cognitive outcome with age and how the group influence this evolution was evaluated with linear mixed effect (LME) models (Oberg and Mahoney, 2007). LME models include both fixed effect (parameters common to an entire population such as age or group) and random effects (subject-specific parameters modeling the subject deviation from the population).

LME was defined to regress each of the network metrics including group, age and the interaction between them as independent variables:

$$y_s=\beta_0+\beta_1\cdot group+\beta_2\cdot age+\beta_3\cdot group\cdot age+\beta_{4,s}+\xi \qquad s=1,\dots,S$$

where $y_s$ is the network metric in the subject $s$ at a given age, $s$ represents each of the $S$ subjects, $\beta_0$ is the global intercept, $\beta_1$, $\beta_2$, $\beta_3$ the fixed effect parameters, assessing the influence of group, age and interaction respectively, and $\beta_{4,s}$ the subject specific correction. $\xi$ is the regression error term.

The group or age effect was considered significant if $p<0.05$. Significant interaction between age and group was defined as $p<0.1$. When the interaction was significant, control and transgenic groups were modeled separately to evaluate the age effect in each group:

$$y_{s_{CTR}}=\beta_{0,CTR}+\beta_{1,CTR}\cdot group+\beta_{2,CTR}\cdot age+\beta_{3,s_{CTR}}+\xi \qquad s_{CTR}=1,\ldots,S_{CTR}$$
$$y_{s_{AD}}=\beta_{0,AD}+\beta_{1,AD}\cdot group+\beta_{2,AD}\cdot age+\beta_{3,s_{AD}}+\xi \qquad s_{AD}=1,\ldots,S_{AD}$$

Finally, the relationship between connectivity and cognitive performance was evaluated fitting an LME model to test if such relation is significant and if it differs between groups:

$$DNMS_s=\beta_0+\beta_1\cdot connectivity+\beta_2\cdot group+\beta_3\cdot connectivity\cdot group+\beta_{4,s}+\xi \qquad s=1,\ldots,S$$

where $DNMS_s$ represents the result in the DNMS task (number of trials or percentage of correct responses) and connectivity refers to a network metric. Thus, the relation between each pair of cognitive outcome and network parameter was evaluated. When interaction was significant ($p<0.1$), the model was fitted separately to AD and control groups to test the significance of the relationship between the network metric and the cognitive outcome in each group.

## 3. Results

### *3.1. Group differences by time points.*

Table 2 compiles the statistically significant differences of network metrics between groups at each of the five acquisition time points. Only network metrics and/or time points where differences were significant are included. Most differences were observed at the earliest time point where most of the structural network metrics were decreased in the transgenic group with respect to controls.

Significant decrease in FA-w clustering coefficient and strength was also present at 8 months of age, and in FA-w local efficiency at 15 months. Regarding the FD-w connectome, while decreased values were observed in the transgenic group with respect to controls at the first time point, a significant increase was detected in strength, global and local efficiency at 9 and 15 months of age, and in clustering coefficient at 15 months of age. No significant differences were found in the functional network metrics.

| ***5.4 months (Time point 1)*** | | | | |
|---|---|---|---|---|
| **Connectome** | **Network metric** | **Control** | **TgF344-AD** | **p-value** |
| FA-weighted | Strength | 16.3683±0.4620 | 14.6515±0.7205 | 0.0033 |
| | Global efficiency | 0.2404±0.0033 | 0.2287±0.0090 | 0.0209 |
| | Clustering coefficient | 0.2262±0.0042 | 0.2134±0.0084 | 0.0086 |
| FD-weighted | Local efficiency | 0.2319±0.0268 | 0.2054±0.0213 | 0.0460 |
| | Clustering coefficient | 0.1279±0.0150 | 0.1128±0.0088 | 0.0357 |
| Structural binary | Degree | 64.0921±2.2237 | 58.5131±2.7763 | 0.0117 |
| | Global efficiency | 0.9273±0.0148 | 0.8901±0.0185 | 0.0117 |
| | Local efficiency | 0.9504±0.0094 | 0.9327±0.0060 | 0.0086 |
| | Clustering coefficient | 0.9009±0.0187 | 0.8654±0.0119 | 0.0086 |
| ***8.2 months (Time point 2)*** | | | | |
| **Connectome** | **Network metric** | **Control** | **TgF344-AD** | **p-value** |
| FA-weighted | Strength | 16.3752±0.3020 | 15.7486±0.9336 | 0.0209 |
| | Clustering coefficient | 0.2319±0.0077 | 0.2253±0.0102 | 0.0433 |
| FD-weighted | Strength | 19.1265±0.3099 | 20.2060±2.1002 | 0.0269 |
| | Global efficiency | 0.7714±0.0454 | 0.8779±0.0669 | 0.0028 |
| | Local efficiency | 0.2126±0.0105 | 0.2286±0.0204 | 0.0209 |
| ***14.9 months (Time point 4)*** | | | | |
| **Connectome** | **Network metric** | **Control** | **TgF344-AD** | **p-value** |
| FA-weighted | Local efficiency | 0.2532±0.0068 | 0.2458±0.0040 | 0.0209 |
| FD-weighted | Strength | 18.1944±4.7926 | 23.1124±1.5442 | 0.0053 |
| | Global efficiency | 0.7514±0.1783 | 0.8818±0.0792 | 0.0269 |
| | Local efficiency | 0.2062±0.0386 | 0.2489±0.0149 | 0.0039 |
| | Clustering coefficient | 0.1160±0.0205 | 0.1388±0.0095 | 0.0039 |

***Table 2.*** Network metrics that showed statistically significant differences between control and transgenic group. Group median and interquartile range in control and TgF344-AD and p-value

resulting from the Kruskal-Wallis test are reported. Only time points/metrics where significant differences were found are included.

Figure 1 shows the group average FA-w and functional weighted connectomes considering only the strongest connections (FA-w>0.3 and z>0.05, respectively). Stronger and denser FA-w connections are observed in the control group in comparison with transgenic, especially in the last time point, although network metrics were not significantly different. A decrease in the connection strength with time in the AD brain can also be observed. Regarding the functional connectome it can be seen that at 18 months of age (T5), z>0.05 connections in the AD brain are less and weaker. In previous time points connectivity is similar between both groups, and even higher strength in specific links can be observed in the AD brain.

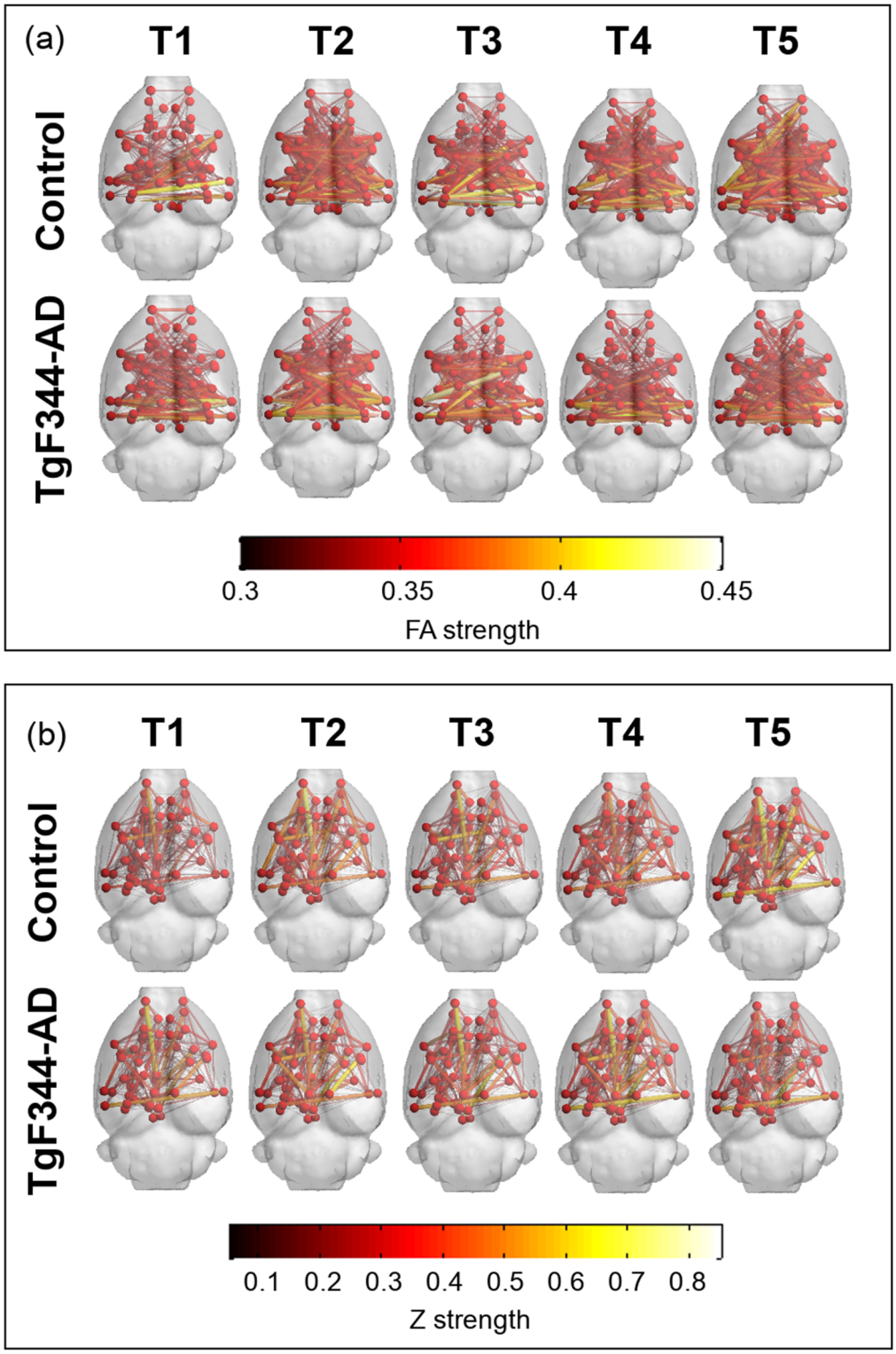


***Figure 1.*** Average structural and functional brain networks. (a) Group average of the FA-w connectome; (b) group average of the functional weighed connectome at each time point. Only the strongest connections are plotted (FA-w>0.3 and z>0.05). Color and width of the links represent connection strength.

Figure 2 shows the DNMS test results. Significant differences were found only in the first time point, when transgenic animals performed less trials than control animals (controls 56.97±13.32, TgF344-AD: 39.4±13.93, p=0.0357). High variability was observed in the AD group results in the last time point, when the performance of some of the animals sharply falls.

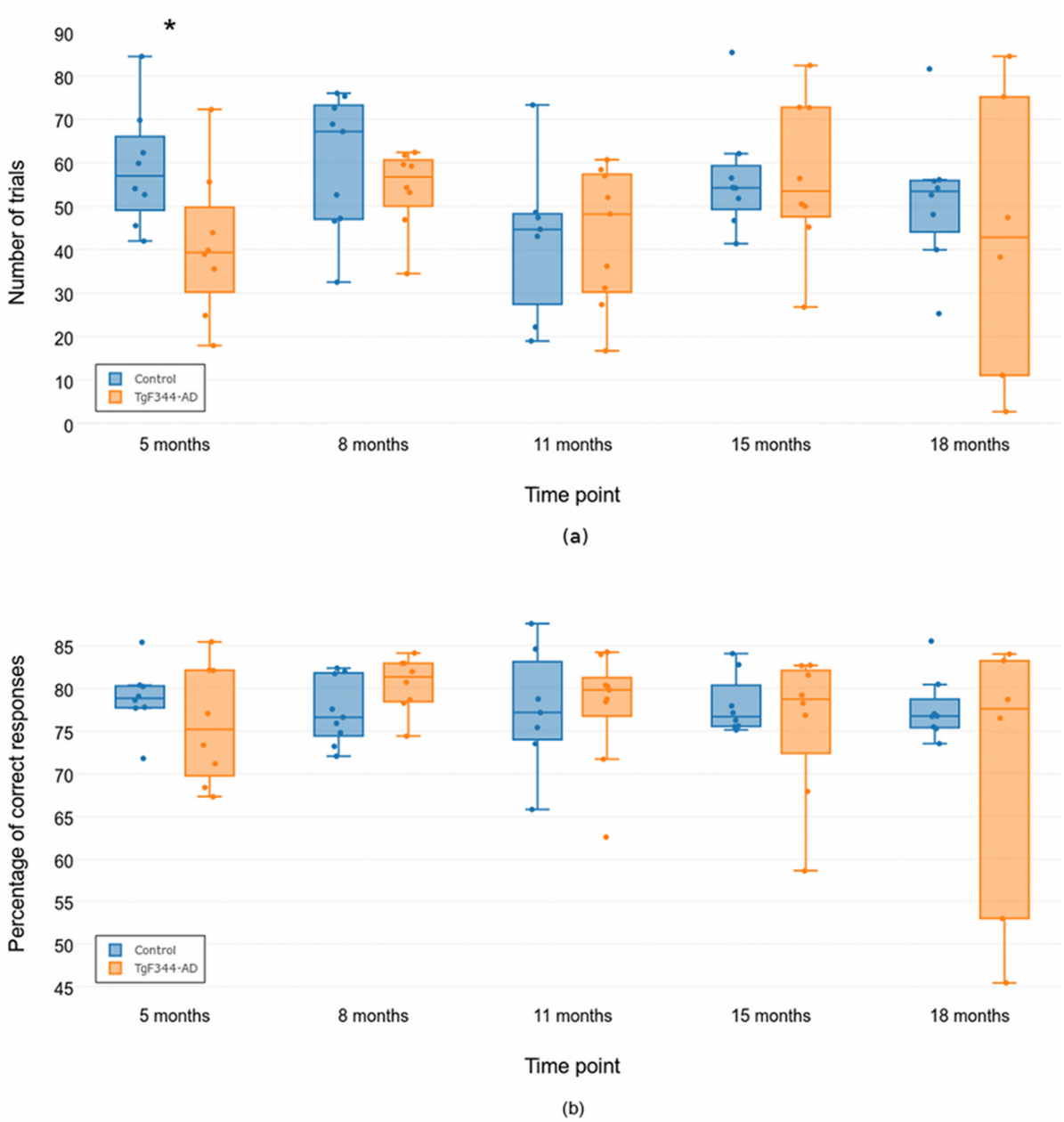


***Figure 2.*** Cognitive performance. (a) Average number of trials per DNMS session and (b) percentage of correct responses in the DNMS task in the five evaluated time points (blue: control group; orange: TgF344-AD group). Asterisk represents significant difference (p<0.05).

### *3.2. Longitudinal analysis*

Linear mixed effect (LME) model was fitted to regress each of the network metrics and to evaluate significant effects of age, group or their interaction. Results are showed in Table 3.

| **Connectome** | **Network metric** | **All subjects** | | | **Control** | **TgF344-AD** |
|---|---|---|---|---|---|---|
| | | Group | Age | GroupxAge | Age | Age |
| FA-weighted | Strength | 0.002 | 0.007 | 0.038 | n.s. | 0.006 |
| | Global efficiency | 0.044 | n.s | n.s. | – | -- |
| | Local efficiency | n.s. | n.s | n.s. | – | – |
| | Clustering coefficient | 0.008 | 0.012 | n.s | -- | -- |
| FD-weighted | Strength | n.s. | 0.043 | 0.010 | n.s. | 0.046 |
| | Global efficiency | n.s. | n.s. | 0.062 | n.s. | 0.023 |
| | Local efficiency | n.s. | n.s. | 0.017 | n.s | n.s |
| | Clustering coefficient | 0.046 | 0.024 | 0.006 | n.s | 0.023 |
| Structural binary | Degree | 0.002 | 0.006 | 0.007 | n.s | 0.012 |
| | Global efficiency | 0.002 | 0.006 | 0.007 | n.s. | 0.012 |
| | Local efficiency | 0.002 | 0.001 | 0.006 | n.s. | 0.003 |
| | Clustering coefficient | 0.002 | 0.001 | 0.006 | n.s. | 0.03 |

***Table 3***. Effect of age, group and age-group interaction in connectivity metrics. p-values of the linear mixed effect model coefficients; significance of group, age and its interaction in the model fitted to all subjects; significance of age effect in the group model (only reported if group-age interaction was considered significant, $p<0.1$)

Figure 3 shows the FA-w, FD-w and binary structural connectome strength/degree and clustering coefficient with respect to age and the model fit. Similar results were obtained for FD-w and binary global and local efficiencies (Figure 4).

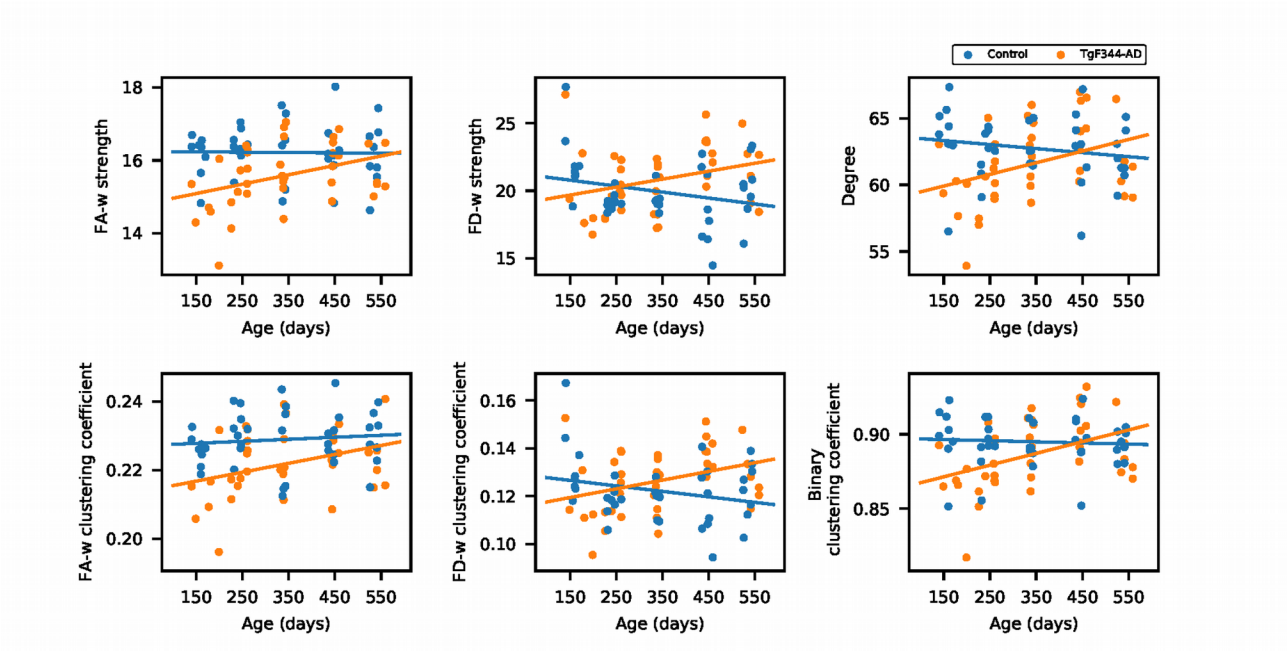


***Figure 3.*** Evolution of network strength, degree and clustering coefficient with age. Linear mixed effect model fit of the network strength, degree and clustering coefficient of the structural connectomes as function of age and group (blue: control, orange: TgF344-AD). Each dot represents the network metric of one animal at one time point.

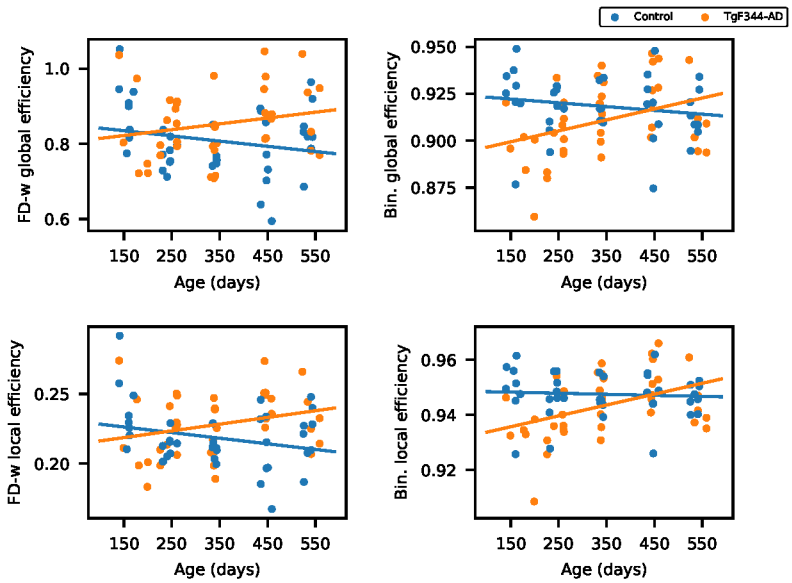


***Figure 4.*** Evolution of network global and local efficiency with age. Linear mixed effect model fit of the network global and local efficiency of the structural connectomes as function of age and

group (blue: control, orange: TgF344-AD). Each dot represents the network metric of one animal at one time point.

In FA-w connectome, although group effect was significant in strength, global efficiency and clustering coefficient, interaction between group and age was only detected in strength, that remains almost constant in the control group while significantly increase with age in AD group.

The interaction between group and age was significant in all the FD-w metrics. All of them, except local efficiency, significantly increase with age in the transgenic group, opposite to the non-significant decrease observed in controls. Similar behavior was observed in the binary connectome: all the network metrics were significantly affected by age in the transgenic group.

No significant effects of age, group or interaction were detected neither in functional connectivity nor in cognitive performance.

### *3.3. Relationship between connectivity and cognition*

The effect of connectivity in cognitive results and if this effect was different in transgenic and control animals was evaluated using LME models.

The interaction between FA-w strength and group had a significant effect in DNMS results. Considering the group specific model, this metric had a significant influence in the number of trials performed by the transgenic animals, but not in controls. Same results were observed considering any of the FD-w or binary metrics. In all the cases, the higher the FD-w or structural binary network metrics, the more trials the transgenic animal performed. Figure 5 shows FA-w, FD-w strength and

structural degree (results are similar in all the mentioned metrics). More details are provided in Table 4.

| | | **Cognitive metric** | | | | | | | | | |
|---|---|---|---|---|---|---|---|---|---|---|---|
| | | **Total trials** | | | | | **Percentage of correct** | | | | |
| | | All subjects | | | CTR | AD | All subjects | | | CTR | AD |
| **Connectome** | **Network metric** | Group effect | Metric effect | Group x metric | Metric | Metric | Group effect | Metric effect | Group x metric | Metric | Metric |
| FA-weighted | Strength | 0.011 | 0.0002 | 0.012 | n.s. | **0.001** | n.s | 0.011 | n.s | – | -- |
| | Global efficiency | n.s. | n.s. | n.s. | -- | -- | n.s | 0.047 | n.s | -- | -- |
| | Clustering coefficient | n.s | 0.007 | n.s | – | – | n.s | 0.016 | n.s | – | -- |
| FD-weighted | Strength | 0.004 | 0.0002 | 0.008 | n.s. | **0.001** | n.s. | n.s. | n.s. | – | -- |
| | Global efficiency | 0.047 | 0.018 | 0.008 | n.s. | **0.046** | n.s. | n.s. | n.s. | – | -- |
| | Local efficiency | 0.003 | 0.0001 | 0.006 | n.s. | **0.0007** | n.s. | n.s. | n.s. | – | -- |
| | Clustering coefficient | 0.001 | 5e-6 | 0.002 | n.s | **3e-5** | n.s | n.s | n.s | -- | -- |
| Structural binary | Degree | 0.001 | 3e-6 | 0.001 | n.s. | **2e-5** | n.s. | 0.036 | n.s. | – | -- |
| | Global efficiency | 0.001 | 3e-6 | 0.001 | n.s. | **2e-5** | n.s. | 0.036 | n.s. | -- | -- |
| | Local efficiency | 0.001 | 4e-6 | 0.001 | n.s. | **2e-6** | n.s. | 0.032 | n.s. | – | -- |
| | Clustering coefficient | 0.001 | 4e-6 | 0.001 | n.s | **2e-6** | n.s | 0.033 | n.s | – | -- |
| Functional weighted | Strength | 0.004 | n.s. | 0.004 | **0.044** | n.s. | 0.02 | n.s. | 0.023 | **0.01** | n.s. |
| | Global efficiency | 0.007 | 0.04 | 0.009 | **0.046** | n.s. | 0.04 | n.s. | 0.044 | n.s. | n.s. |
| | Local efficiency | n.s. | n.s. | n.s. | -- | -- | n.s. | n.s. | 0.06 | **0.032** | n.s. |
| | Clustering coefficient | n.s. | n.s. | 0.092 | n.s. | n.s. | n.s. | n.s. | n.s. | – | -- |

***Table 4.*** Effect of network metrics and group in cognitive performance. p-values of the linear mixed effect model coefficients regressing cognitive outcome (total number of trials and percentage of

correct response) by group, network metric and their interaction. Significance of group, network metric and interaction of the LME model fitted to all subjects; significance of network metric effect in cognitive outcome when group-specific LME model was fitted to each group (only reported if group-age interaction was significant, p<0.1). Only metrics with significant effects are included.

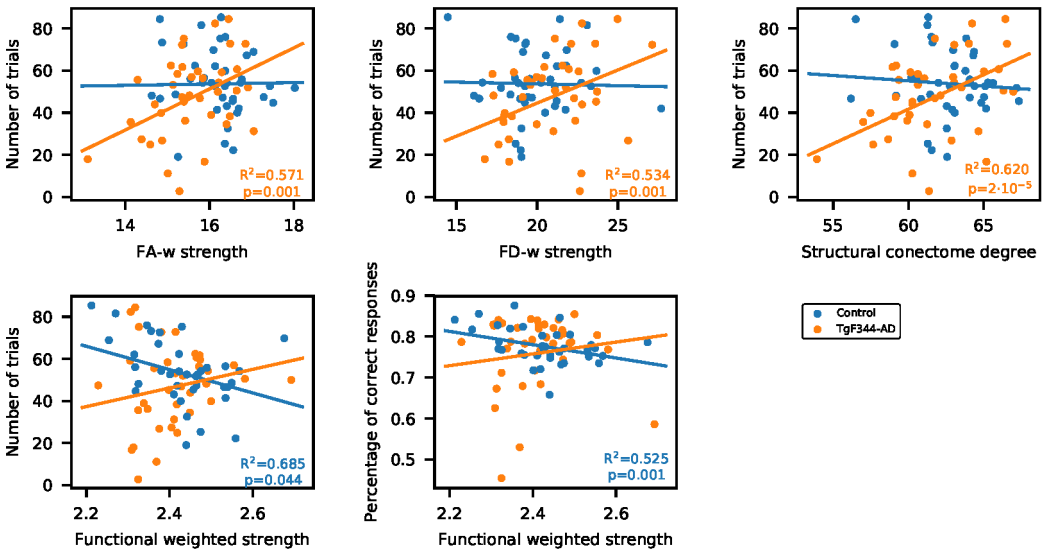


***Figure 5***. Cognitive performance and network metrics. Linear mixed model fit of DNMS result as function of network metric and group. First row, relationship between the structural connectome metrics and number of trials performed in DNMS test; second row: relationship between functional connectome metrics and number of trials/percentage of correct response in DNMS. R-squared and p-value in case of significant metric effect (orange: significance in TgF344-AD group; blue: significance in control group).

The number of trials was significantly influenced by the interaction between group and functional weighted global efficiency or strength, while the percentage of correct responses was significantly affected by the interaction between group and functional local efficiency and strength. In all these cases, when specific group models were considered, the effect of these metrics in the cognitive performance was significant in the control animals, but not in the transgenic cohort.

## 4. Discussion

In this study, structural and functional network changes during the progression of AD have been evaluated using MRI-based connectomics applied to a rat model of AD. Differences in the structural brain network between population at risk of AD or in its preclinical phases in human cohorts have been already reported (Berlot et al., 2016; Chen et al., 2015; Farrar et al., 2017; Fischer et al., 2015; Pereira et al., 2017; Zhao et al., 2015). In our study, the evaluation of the structural brain network in TgF344-AD from ages corresponding to earlier stages than the ones covered in human studies pointed to similar connectivity changes already in young animals (six months of age). These differences were also observed later in time, together with a different evolution of the structural metrics. While aging had no significant effect in the evolution of network metrics in the control group, it significantly affected to metrics in the transgenic animals. In this group, metrics increased linearly with age, but a decrease in the metric values at the last time point can be observed in Figure 3 and 4, although LME could not fit this change of trend. In spite of this global increment with age, FA-w network metrics in transgenic animal remain always lower than in controls, in line with which has been observed in preclinical or clinical phases of AD in patients (Chen et al., 2015; Pereira et al., 2017; Shu et al., 2015). However, binary and FD-w metrics were decreased with respect to controls in the first time points but FD-w was significantly increased in transgenic at 8 and 15 months. This could be related with the hyperconnectivity effect described after brain injury and in preclinical phases of AD (Hillary and Grafman, 2017), explained as a mechanism to preserve communication in the network and minimize the behavioral deficits. Although hyperconnectivity has been mainly identified in functional networks, higher binary structural network properties were also described in *APOE* ε4 carriers before MCI appears (Ma et al., 2017). Thus, to compensate the lower FA-w strength in the network, more connections would be established to preserve behavioral performance. In this line, the increase in FA-w network metrics with age observed in transgenic

animals is probably related to the presence of more connections rather than to FA increase in the brain.

Impairments in functional connectivity have been described in at risk, preclinical or clinical AD cohorts, but depending on methodological issues or cohort selection differences have been reported in opposed senses (Phillips et al., 2015). Likewise, in the studied animal model, TgF377-AD, differences in connectivity between specific regions have been reported (Anckaerts et al., 2019) at several ages. In the present work, we focused on the analysis of brain network globally instead of evaluation specific connections. From this point of view, the whole-brain network metrics describing integration and segregation of the functional connectomes did not significantly differ between control and transgenic groups. This could be related to three factors. First, the hyperconnectivity effect previously mentioned (Hillary and Grafman, 2017) between specific regions or networks to compensate damaged connections (hypoconnectivity). This effect has been described, for instance, in young *APOE* ε4 carriers (Ma et al., 2017) or amnestic MCI patients (Kim et al., 2015). Therefore, decreased connections would be compensated by increased connections, resulting in similar values of the global network metrics evaluated in our study. Second, the training and the repetition of the cognitive task could lead to a learning effect, increasing the cognitive reserve of these animals and therefore preserving the functional connectivity. Higher functional connectivity has been related with higher cognitive reserve in both healthy elders (Arenaza-Urquijo et al., 2013) and MCI patients (Franzmeier et al., 2017) with respect to subjects with low cognitive reserve. This fact could also be related with the absence of significant differences in the cognitive outcome. Nevertheless, further investigation on animals not undergoing DNMS should be performed to confirm this hypothesis. Finally, the third factor that could influence the absence of functional connectivity differences could be the timing of the disease. Brain changes as amyloid-β concentration and neural loss in TgF344-AD have been described from 16 months of age (Cohen et

al., 2013) and significant cognitive impairment is mainly described from 15 months (Cohen et al., 2013; Tsai et al., 2014) although tendencies to impairment or differences in anxiety or learning abilities have been reported at earlier stages (Cohen et al., 2013; Muñoz-Moreno et al., 2018; Pentkowski et al., 2018). Actually, in Figure 2 it can be observed that cognitive performance was similar between both groups at all the time points, but an increase in variability appeared at 18 months of age, when some of the transgenic animals performed much worse than at previous ages. This suggests that the symptomatic onset occurs around 18 months of age, and before this age, functional connectivity might compensate the structural network damage resulting in similar functional network metrics than in control animals. The observed significant relation between structural network metrics and cognitive performance could be related with the ability of functional connectivity to cope with the structural disconnection preserving cognition, until a breakpoint when it is not able to deal with extensive structural network damage. This relationship between structural connectivity and cognition has been also described in MCI subjects (Berlot et al., 2016; Farrar et al., 2017) and in cognitive normal individuals harboring amyloid pathology and neurodegeneration (Pereira et al., 2017), while no correlation was observed in control subjects. Coherently, structural connectivity did not correlate with DNMS in our control cohort, where correlation between DNMS and functional connectivity was observed.

***Strengths and limitations***

The use of MRI-based connectomics to longitudinally analyse the brain network in an animal model of AD provides a valuable and highly translational approach to the research on the mechanism of the disease progression, since the applied methodology can be easily translated to clinical investigation. Besides, the use of animals models allows for characterization and follow-up of the same cohort from early stages until advanced phases of AD. Indeed, the model used in our

experiments, the Tg344-AD rats, has been shown to develop all the AD pathological hallmarks in a progressive manner, which makes it specially suitable for longitudinal evaluation.

The proposed methodology allows for comparison between the results followed and previous results published describing connectivity changes in human cohorts. Thus, our results are coherent with those observed in human studies as aforementioned, and provide new insights into the evolution of disconnection associated to the progression of AD. Furthermore, the use of a rat model allows for better behavioral characterization than other animal models (Do Carmo and Cuello, 2013). This makes possible to perform cognitive evaluation of memory related functions and relate animal performance with brain connectivity. Hence, brain network organization influence in cognitive abilities differs between transgenic and control animals.

Regarding the limitations of the study, the relatively small number of subjects could limit the statistical analysis. However, measures were repeated at 5 time points, which increases the sample size evaluated by the longitudinal models. Notwithstanding, the results obtained from the statistical analysis were coherent with previous findings observed in bigger cohorts from human population. Furthermore, we would like to mention that all animals in the study repeated the DNMS task every three months, which allows for evaluation of cognitive skills. Results point to a learning effect and increase in cognitive reserve due to such repetition. However, further experiments which include animals not performing DNMS should be carried out for more thorough evaluation of such an effect.

Finally, the last time point evaluated in our study is 18 months of age. Brain changes and cognitive impairment in the TgF344-AD has been described mainly from 15 months of age, what, as previously discussed, could be related with the absence of differences in cognition or functional

connectivity. Therefore, further investigation describing connectivity at later time points would be of great interest to characterize more advanced stages of the disease.

## 5. Conclusions

The connectivity analysis of TgF344-AD rats not only replicates results observed in human populations at risk of AD, but it allows to characterize earlier stages of the disease and follow up its progression to identify breaking points in network evolution. The results support the idea of AD as a continuum, pointing to brain damage already present at early stages, long before the symptomatic onset. These alterations lead to a pattern of brain changes during aging associated to the disease, which differs from evolution in the control cohort. Likewise, impairments in structural brain network are in line with the hypothesis of AD as a disconnection syndrome. The impact of the altered anatomical connectivity in cognitive skills could be moderated by functional network reorganization until advanced stages of the disease. This suggests the relevance of cognitive reserve to prevent or mitigate the symptomatic onset in subjects affected by the disease.

**Acknowledgements**

This work was supported the Plan Nacional I+D+I and co-funded by ISCIII-Subdirección General de Evaluación and European Regional Development Fund (ERDF) [grant number: PI14/00595]; and by the Fundació La Marató de TV3 [grant number 201441 10]. Consorcio Centro de Investigación Biomédica en Red (CIBER) de Bioingeniería, Biomateriales y Nanomedicina (CIBER-BBN) is an initiative financed by the Instituto de Salud Carlos III with assistance from the European Regional Development Fund. The work was also funded by InMind project financed by the European Community [grant number: FP7-HEALTH-2011.2.2.1-2, nº 278850]. TgF344-AD rats were obtain through the InMind Consortium following kind donation by Dr. T Town.

We are indebted to the Experimental MRI 7T Unit of the Institut d'Investigacions Biòmediques August Pi i Sunyer.

## References

Anckaerts, C., Blockx, I., Summer, P., Michael, J., Hamaide, J., Kreutzer, C., Boutin, H., Couillard-Després, S., Verhoye, M., Van der Linden, A., 2019. Early functional connectivity deficits and progressive microstructural alterations in the TgF344-AD rat model of Alzheimer's Disease: A longitudinal MRI study. Neurobiol. Dis. 124, 93–107. https://doi.org/10.1016/j.nbd.2018.11.010

Arenaza-Urquijo, E.M., Landeau, B., La Joie, R., Mevel, K., Mézenge, F., Perrotin, A., Desgranges, B., Bartrés-Faz, D., Eustache, F., Chételat, G., 2013. Relationships between years of education and gray matter volume, metabolism and functional connectivity in healthy elders. Neuroimage 83, 450–457. https://doi.org/10.1016/j.neuroimage.2013.06.053

Badhwar, A.P., Tam, A., Dansereau, C., Orban, P., Hoffstaedter, F., Bellec, P., 2017. Resting-state network dysfunction in Alzheimer's disease: A systematic review and meta-analysis. Alzheimer's Dement. Diagnosis, Assess. Dis. Monit. 8, 73–85. https://doi.org/10.1016/j.dadm.2017.03.007

Berlot, R., Metzler-Baddeley, C., Ikram, M.A., Jones, D.K., O'Sullivan, M.J., 2016. Global efficiency of structural networks mediates cognitive control in mild cognitive impairment. Front. Aging Neurosci. 08, 292. https://doi.org/10.3389/fnagi.2016.00292

Brier, M.R., Thomas, J.B., Ances, B.M., 2014a. Network dysfunction in Alzheimer's disease: refining the disconnection hypothesis. Brain Connect. 4, 299–311. https://doi.org/10.1089/brain.2014.0236

Brier, M.R., Thomas, J.B., Fagan, A.M., Hassenstab, J., Holtzman, D.M., Benzinger, T.L., Morris, J.C., Ances, B.M., 2014b. Functional connectivity and graph theory in preclinical Alzheimer's disease. Neurobiol. Aging 35, 757–768. https://doi.org/10.1016/j.neurobiolaging.2013.10.081

Cacciaglia, R., Molinuevo, J.L., Falcón, C., Brugulat-Serrat, A., Sánchez-Benavides, G., Gramunt, N., Esteller, M., Morán, S., Minguillón, C., Fauria, K., Gispert, J.D., 2018. Effects of APOE-ε4 allele load on brain morphology in a cohort of middle-aged healthy individuals with enriched genetic risk for Alzheimer's disease. Alzheimer's Dement. 14, 902–912. https://doi.org/10.1016/j.jalz.2018.01.016

Chen, Y., Chen, K., Zhang, J., Li, X., Shu, N., Wang, J., Zhang, Z., Reiman, E.M., 2015. Disrupted functional and structural networks in cognitively normal elderly subjects with the APOE ε4 allele. Neuropsychopharmacology 40, 1181–1191. https://doi.org/10.1038/npp.2014.302

Cohen, R.M., Rezai-Zadeh, K., Weitz, T.M., Rentsendorj, A., Gate, D., Spivak, I., Bholat, Y., Vasilevko, V., Glabe, C.G., Breunig, J.J., Rakic, P., Davtyan, H., Agadjanyan, M.G., Kepe, V.,

Barrio, J., Bannykh, S., Szekely, C.A., Pechnick, R.N., Town, T.C., 2013. A transgenic Alzheimer rat with plaques, tau pathology, behavioral impairment, oligomeric Aβ and frank neuronal loss. J. Neurosci. 33, 6245–6256. https://doi.org/10.1523/JNEUROSCI.3672-12.2013

Daianu, M., Jahanshad, N., Nir, T.M., Toga, A.W., Jack, C.R., Weiner, M.W., Thompson, P.M., Initiative, A.D.N., 2013. Breakdown of brain connectivity between normal aging and Alzheimer's disease: a structural k-core network analysis. Brain Connect. 3, 407–22. https://doi.org/10.1089/brain.2012.0137

Do Carmo, S., Cuello, A.C., 2013. Modeling Alzheimer's disease in transgenic rats. Mol. Neurodegener. 8, 37. https://doi.org/10.1186/1750-1326-8-37

Drummond, E., Wisniewski, T., 2017. Alzheimer's disease: experimental models and reality. Acta Neuropathol. 133, 155–175. https://doi.org/10.1007/s00401-016-1662-x

Dubois, B., Hampel, H., Feldman, H.H., Scheltens, P., Aisen, P., Andrieu, S., Bakardjian, H., Benali, H., Bertram, L., Blennow, K., Broich, K., Cavedo, E., Crutch, S., Dartigues, J.F., Duyckaerts, C., Epelbaum, S., Frisoni, G.B., Gauthier, S., Genthon, R., Gouw, A.A., Habert, M.O., Holtzman, D.M., Kivipelto, M., Lista, S., Molinuevo, J.L., O'Bryant, S.E., Rabinovici, G.D., Rowe, C., Salloway, S., Schneider, L.S., Sperling, R., Teichmann, M., Carrillo, M.C., Cummings, J., Jack, C.R., 2016. Preclinical Alzheimer's disease: Definition, natural history, and diagnostic criteria. Alzheimer's Dement. 12, 292–323. https://doi.org/10.1016/j.jalz.2016.02.002

Farrar, D.C., Mian, A.Z., Budson, A.E., Moss, M.B., Koo, B.B., Killiany, R.J., 2017. Retained executive abilities in mild cognitive impairment are associated with increased white matter network connectivity. Eur. Radiol. 340–347. https://doi.org/10.1007/s00330-017-4951-4

Fischer, F.U., Wolf, D., Scheurich, A., Fellgiebel, A., 2015. Altered whole-brain white matter networks in preclinical Alzheimer's disease. NeuroImage Clin. 8, 660–666. https://doi.org/10.1016/j.nicl.2015.06.007

Franzmeier, N., Caballero, M.Á.A., Taylor, A.N.W., Simon-Vermot, L., Buerger, K., Ertl-Wagner, B., Mueller, C., Catak, C., Janowitz, D., Baykara, E., Gesierich, B., Duering, M., Ewers, M., 2017. Resting-state global functional connectivity as a biomarker of cognitive reserve in mild cognitive impairment. Brain Imaging Behav. 11, 368–382. https://doi.org/10.1007/s11682-016-9599-1

Frisoni, G.B., Fox, N.C., Jack, C.R., Scheltens, P., Thompson, P.M., 2010. The clinical use of structural MRI in Alzheimer disease. Nat. Rev. Neurol. 6, 67–77. https://doi.org/10.1038/nrneurol.2009.215

Galeano, P., Martino Adami, P. V, Do Carmo, S., Blanco, E., Rotondaro, C., Capani, F., Castaño, E.M., Cuello, A.C., Morelli, L., 2014. Longitudinal analysis of the behavioral phenotype in a novel transgenic rat model of early stages of Alzheimer's disease. Front. Behav. Neurosci. 8, 321. https://doi.org/10.3389/fnbeh.2014.00321

Gomez-Ramirez, J., Wu, J., 2014. Network-based biomarkers in Alzheimer's disease: Review and future directions. Front. Aging Neurosci. 6, 12. https://doi.org/10.3389/fnagi.2014.00012

Gour, N., Felician, O., Didic, M., Koric, L., Gueriot, C., Chanoine, V., Confort-Gouny, S., Guye, M., Ceccaldi, M., Ranjeva, J.P., 2014. Functional connectivity changes differ in early and late-onset Alzheimer's disease. Hum. Brain Mapp. 35, 2978–2994. https://doi.org/10.1002/hbm.22379

Habib, M., Mak, E., Gabel, S., Su, L., Williams, G.B., Waldman, A., Wells, K., Ritchie, K., Ritchie, C., O'Brien, J.T., 2017. Functional neuroimaging findings in healthy middle-aged adults at risk of Alzheimer's disease. Ageing Res. Rev. 36, 88–104. https://doi.org/10.1016/j.arr.2017.03.004

Hillary, F.G., Grafman, J.H., 2017. Injured brains and adaptive networks: The benefits and costs of hyperconnectivity. Trends Cogn. Sci. 21, 385–401. https://doi.org/10.1016/j.tics.2017.03.003

Jack, C.R., Barnes, J., Bernstein, M.A., Borowski, B.J., Brewer, J., Clegg, S., Dale, A.M., Carmichael, O., Ching, C., DeCarli, C., Desikan, R.S., Fennema-Notestine, C., Fjell, A.M., Fletcher, E., Fox, N.C., Gunter, J., Gutman, B.A., Holland, D., Hua, X., Insel, P., Kantarci, K., Killiany, R.J., Krueger, G., Leung, K.K., Mackin, S., Maillard, P., Malone, I.B., Mattsson, N., McEvoy, L., Modat, M., Mueller, S., Nosheny, R., Ourselin, S., Schuff, N., Senjem, M.L., Simonson, A., Thompson, P.M., Rettmann, D., Vemuri, P., Walhovd, K.B., Zhao, Y., Zuk, S., Weiner, M.W., 2015. Magnetic resonance imaging in Alzheimer's Disease Neuroimaging Initiative 2. Alzheimer's Dement. 11, 740–756. https://doi.org/10.1016/j.jalz.2015.05.002

Jack, C.R., Bennett, D.A., Blennow, K., Carrillo, M.C., Dunn, B., Haeberlein, S.B., Holtzman, D.M., Jagust, W.J., Jessen, F., Karlawish, J., Liu, E., Molinuevo, J.L., Montine, T., Phelps, C., Rankin, K.P., Rowe, C.C., Scheltens, P., Siemers, E., Snyder, H.M., Sperling, R., Elliott, C., Masliah, E., Ryan, L., Silverberg, N., 2018. NIA-AA Research Framework: Toward a biological definition of Alzheimer's disease. Alzheimer's Dement. 14, 535–562. https://doi.org/10.1016/j.jalz.2018.02.018

Kim, H., Yoo, K., Na, D.L., Seo, S.W., Jeong, J., Jeong, Y., 2015. Non-monotonic reorganization of brain networks with Alzheimer's disease progression. Front. Aging Neurosci. 7, 1–10. https://doi.org/10.3389/fnagi.2015.00111

Leon, W.C., Canneva, F., Partridge, V., Allard, S., Ferretti, M.T., DeWilde, A., Vercauteren, F., Atifeh, R., Ducatenzeiler, A., Klein, W., Szyf, M., Alhonen, L., Cuello, a C., 2010. A novel transgenic rat model with a full Alzheimer's-like amyloid pathology displays pre-plaque intracellular amyloid-beta-associated cognitive impairment. J. Alzheimers. Dis. 20, 113–126. https://doi.org/10.3233/JAD-2010-1349

Lo, C., Wang, P., Chou, K., Wang, J., He, Y., Lin, C., 2010. Diffusion tensor tractography reveals abnormal topological organization in structural cortical networks in Alzheimer's disease. J. Neurosci. 30, 16876–16885. https://doi.org/10.1523/JNEUROSCI.4136-10.2010

Ma, C., Wang, J., Zhang, J., Chen, K., Li, X., Shu, N., Chen, Y., Liu, Z., Zhang, Z., 2017. Disrupted brain structural connectivity: Pathological interactions between genetic APOE ε4 status and

developed MCI condition. Mol. Neurobiol. 54, 6999–7007. https://doi.org/10.1007/s12035-016-0224-5

Mak, E., Gabel, S., Mirette, H., Su, L., Williams, G.B., Waldman, A., Wells, K., Ritchie, K., Ritchie, C., O'Brien, J., 2017. Structural neuroimaging in preclinical dementia: From microstructural deficits and grey matter atrophy to macroscale connectomic changes. Ageing Res. Rev. 35, 250–264. https://doi.org/10.1016/j.arr.2016.10.001

Muñoz-Moreno, E., Tudela, R., López-Gil, X., Soria, G., 2018. Early brain connectivity alterations and cognitive impairment in a rat model of Alzheimer's disease. Alzheimers. Res. Ther. 10, 16. https://doi.org/10.1186/s13195-018-0346-2

Oberg, A.L., Mahoney, D.W., 2007. Linear mixed effects models, in: Methods in Molecular Biology: Topics in Biostatistics. pp. 213–234. https://doi.org/10.1007/978-1-59745-530-5_11

Palesi, F., Castellazzi, G., Casiraghi, L., Sinforiani, E., Vitali, P., Wheeler-Kingshott, C.A.G., Angelo, E.D., 2016. Exploring patterns of alteration in Alzheimer's disease brain networks: a combined structural and functional connectomics analysis. Front. Neurosci. 10, 380. https://doi.org/10.3389/fnins.2016.00380

Pentkowski, N.S., Berkowitz, L.E., Thompson, S.M., Drake, E.N., Olguin, C.R., Clark, B.J., 2018. Anxiety-like behavior as an early endophenotype in the TgF344-AD rat model of Alzheimer's disease. Neurobiol. Aging 61, 169–176. https://doi.org/10.1016/j.neurobiolaging.2017.09.024

Pereira, J.B., van Westen, D., Stomrud, E., Strandberg, T.O., Volpe, G., Westman, E., Hansson, O., 2017. Abnormal structural brain connectome in individuals with preclinical Alzheimer's disease. Cereb. Cortex 28, 3638–3649. https://doi.org/10.1093/cercor/bhx236

Phillips, D.J., McGlaughlin, A., Ruth, D., Jager, L.R., Soldan, A., 2015. Graph theoretic analysis of structural connectivity across the spectrum of Alzheimer's disease: The importance of graph creation methods. NeuroImage Clin. 7, 377–390. https://doi.org/10.1016/j.nicl.2015.01.007

Power, J.D., Plitt, M., Laumann, T.O., Martin, A., 2017. Sources and implications of whole-brain fMRI signals in humans. Neuroimage 146, 609–625. https://doi.org/10.1016/j.neuroimage.2016.09.038

Reiter, K., Nielson, K.A., Durgerian, S., Woodard, J.L., Smith, J.C., Seidenberg, M., Kelly, D.A., Rao, S.M., 2017. Five-Year longitudinal brain volume change in healthy elders at genetic risk for Alzheimer's disease. J. Alzheimer's Dis. 55, 1363–1377. https://doi.org/10.3233/JAD-160504

Rubinov, M., Sporns, O., 2010. Complex network measures of brain connectivity: uses and interpretations. Neuroimage 52, 1059–1069. https://doi.org/10.1016/j.neuroimage.2009.10.003

Sabbagh, J.J., Kinney, J.W., Cummings, J.L., 2013. Alzheimer's disease biomarkers in animal models: closing the translational gap. Am. J. Neurodegener. Dis. 2, 108–120.

Sanz-Arigita, E.J., Schoonheim, M.M., Damoiseaux, J.S., Rombouts, S.A.R.B., Maris, E., Barkhof, F., Scheltens, P., Stam, C.J., 2010. Loss of "small-world" networks in Alzheimer's disease:

graph analysis of fMRI resting-state functional connectivity. PLoS One 5, e13788. https://doi.org/10.1371/journal.pone.0013788

Schwarz, A.J., Gozzi, A., Reese, T., Bifone, A., 2007. In vivo mapping of functional connectivity in neurotransmitter systems using pharmacological MRI. Neuroimage 34, 1627–1636. https://doi.org/10.1016/j.neuroimage.2006.11.010

Shu, N., Li, X., Ma, C., Zhang, J., Chen, K., Liang, Y., Chen, Y., Zhang, Z., 2015. Effects of APOE promoter polymorphism on the topological organization of brain structural connectome in nondemented elderly. Hum. Brain Mapp. 36, 4847–4858. https://doi.org/10.1002/hbm.22954

Supekar, K., Menon, V., Rubin, D., Musen, M., Greicius, M.D., 2008. Network analysis of intrinsic functional brain connectivity in Alzheimer's disease. PLoS Comput. Biol. 4, e1000100. https://doi.org/10.1371/journal.pcbi.1000100

ten Kate, M., Sanz-Arigita, E.J., Tijms, B.M., Wink, A.M., Clerigue, M., Garcia-Sebastian, M., Izagirre, A., Ecay-Torres, M., Estanga, A., Villanua, J., Vrenken, H., Visser, P.J., Martinez-Lage, P., Barkhof, F., 2016. Impact of APOE-ε4 and family history of dementia on gray matter atrophy in cognitively healthy middle-aged adults. Neurobiol. Aging 38, 14–20. https://doi.org/10.1016/j.neurobiolaging.2015.10.018

Tsai, Y., Lu, B., Ljubimov, A. V, Girman, S., Ross-Cisneros, F.N., Sadun, A.A., Svendsen, C.N., Cohen, R.M., Wang, S., 2014. Ocular changes in TGF344-AD rat model of Alzheimer's disease. Investig. Ophthalmol. Vis. Sci. 55, 523–534. https://doi.org/10.1167/iovs.13-12888

Valdés-Hernández, P.A., Sumiyoshi, A., Nonaka, H., Haga, R., Aubert-Vásquez, E., Ogawa, T., Iturria-Medina, Y., Riera, J.J., Kawashima, R., 2011. An in vivo MRI template set for morphometry, tissue segmentation, and fMRI localization in rats. Front. Neuroinform. 5, 26. https://doi.org/10.3389/fninf.2011.00026

Wee, C.-Y., Yap, P.-T., Li, W., Denny, K., Browndyke, J.N., Potter, G.G., Welsh-Bohmer, K.A., Wang, L., Shen, D., 2011. Enriched white matter connectivity networks for accurate identification of MCI patients. Neuroimage 54, 1812–22. https://doi.org/10.1016/j.neuroimage.2010.10.026

Weston, P.S.J., Simpson, I.J.A., Ryan, N.S., Ourselin, S., Fox, N.C., 2015. Diffusion imaging changes in grey matter in Alzheimer's disease: a potential marker of early neurodegeneration. Alzheimers. Res. Ther. 7, 47. https://doi.org/10.1186/s13195-015-0132-3

Windisch, M., 2014. We can treat Alzheimer's disease successfully in mice but not in men: Failure in translation? A perspective. Neurodegener. Dis. 13, 147–150. https://doi.org/10.1159/000357568

Xie, T., He, Y., 2012. Mapping the Alzheimer's brain with connectomics. Front. Psychiatry 2, 77. https://doi.org/10.3389/fpsyt.2011.00077

Zhao, T., Cao, M., Niu, H., Zuo, X.-N., Evans, A.C., He, Y., Dong, Q., Shu, N., 2015. Age-related changes in the topological organization of the white matter structural connectome across the human lifespan. Hum. Brain Mapp. 36, 3777–3792. https://doi.org/10.1002/hbm.22877